Test and Evaluation of Solar Foil Directly Mounted on the Ground

Cooperative Research and Development Final Report

CRADA Number: CRD-19-00793

NREL Technical Contact: Paul Ndione

NREL is a national laboratory of the U.S. Department of Energy
Office of Energy Efficiency & Renewable Energy
Operated by the Alliance for Sustainable Energy, LLC

This report is available at no cost from the National Renewable Energy Laboratory (NREL) at www.nrel.gov/publications.

Contract No. DE-AC36-08GO28308

Technical Report
NREL/TP-5700-84844
December 2022

Test and Evaluation of Solar Foil Directly Mounted on the Ground

Cooperative Research and Development Final Report

CRADA Number: CRD-19-00793

NREL Technical Contact: Paul Ndione

Suggested Citation
Ndione, Paul. 2022. *Test and Evaluation of Solar Foil Directly Mounted on the Ground: Cooperative Research and Development Final Report, CRADA Number CRD-19-00793.* Golden, CO: National Renewable Energy Laboratory. NREL/TP-5700-84844. https://www.nrel.gov/docs/fy23osti/84844.pdf.

NREL is a national laboratory of the U.S. Department of Energy
Office of Energy Efficiency & Renewable Energy
Operated by the Alliance for Sustainable Energy, LLC

This report is available at no cost from the National Renewable Energy Laboratory (NREL) at www.nrel.gov/publications.

Contract No. DE-AC36-08GO28308

Technical Report
NREL/TP-5700-84844
December 2022

National Renewable Energy Laboratory
15013 Denver West Parkway
Golden, CO 80401
303-275-3000 • www.nrel.gov

NOTICE

This work was authored by the National Renewable Energy Laboratory, operated by Alliance for Sustainable Energy, LLC, for the U.S. Department of Energy (DOE) under Contract No. DE-AC36-08GO28308. Funding provided U.S. Department of Energy Office of Energy Efficiency and Renewable Energy Solar Energy Technologies Office. The views expressed herein do not necessarily represent the views of the DOE or the U.S. Government.

This report is available at no cost from the National Renewable Energy Laboratory (NREL) at www.nrel.gov/publications.

U.S. Department of Energy (DOE) reports produced after 1991 and a growing number of pre-1991 documents are available free via www.OSTI.gov.

Cover Photos by Dennis Schroeder: (clockwise, left to right) NREL 51934, NREL 45897, NREL 42160, NREL 45891, NREL 48097, NREL 46526.

NREL prints on paper that contains recycled content.

Cooperative Research and Development Final Report

Report Date: December 16, 2022

In accordance with requirements set forth in the terms of the CRADA agreement, this document is the CRADA final report, including a list of subject inventions, to be forwarded to the DOE Office of Scientific and Technical Information as part of the commitment to the public to demonstrate results of federally funded research.

Parties to the Agreement: HyET Solar BV

CRADA Number: CRD-19-00793

CRADA Title: Test and Evaluation of Solar Foil Directly Mounted on the Ground

Responsible Technical Contact at Alliance/National Renewable Energy Laboratory (NREL):

Paul Ndione | paul.ndione@nrel.gov

Contributors: Peter Hacke, Bill Marion, Bill Sekulic, Kent Terwilliger, Byron MacDanold, Joshua Parker

Name and Email Address of POC at Company:

Rombout Swanborn, CEO | rombout.swanborn@hyet.nl

Contributors: Alexis Dubois, Quentin Swanborn

Sponsoring DOE Program Office(s):

Office of Energy Efficiency and Renewable Energy (EERE), Solar Energy Technologies Office (SETO)

Joint Work Statement Funding Table showing DOE commitment:

No NREL Shared Resources

Estimated Costs	NREL Shared Resources a/k/a Government In-Kind
Year 1	$0.00
TOTALS	$0.00

Executive Summary of CRADA Work:

HyET Solar (HyET), established in 2012, is a small business developing a thin-film silicon solar photovoltaic (PV) product called "Power Foil" that can be mounted directly on the constructed earthen dykes. HyET's goals are for low-cost, efficient, generation of PV electricity at utility scale. HyET has requested assistance from the National Renewable Energy Laboratory (NREL) to evaluate the performance of the Power Foil product in several outdoor environments, with a particular focus on 1) heat effects on efficiency and 2) heat and UV effects on reliability and durability. NREL has been working on PV module testing at laboratory scale for more than 40 years, and has the equipment and facilities required to provide the PV material testing required.

CRADA benefit to DOE, Participant, and US Taxpayer:

- Assists laboratory in achieving programmatic scope
- Enhances the laboratory's core competencies, and/or
- Uses the laboratory's core competencies

Summary of Research Results:

1. Task 1: Equilibrium temperature of PV material mounted on ground:

1.1. Description of Task 1

NREL will engage in experimental validation utilizing 30 cm mini-modules mounted on the ground in NREL's outdoor test facility (OTF). Each mini-module will have embedded temperature sensors. NREL's facilities have appropriate metrological and irradiance data collection capabilities. Data will be collected using 5-15-minute collection intervals for approximately two months. Data on ambient temperature, humidity, wind speed, irradiance, soil temperatures, and module temperatures will be fed back into the computational models to optimize model accuracy.

1.2. Task 1 Results

1.2.1. Design Validation and Preparation.

PV Reliability Group helped HyET engineers develop two phases of testing to validate their module designs and backsheet membrane in a pseudo desert environment. NREL and HyET developed a statement of work, job plan and work breakdown structure to accomplish these project goals.

1.2.2. Testing Setup

The first testing scenario, an 8-module laminate temperature test was setup to verify temperature profiles in fielded laminated modules and backing. The test incorporated 8 non-functional modules, approximately 14 thermocouple temperature sensors and data gathering equipment. PV Reliability engineers and technicians designed the testing apparatus and helped HyET engineers install and calibrate the sensors and logger. This test collected data for a few weeks and helped shape the next round of testing of 32 modules.The second testing scenario involved 32 HyET modules. A field testbed was designed and built by NREL Engineers and Technicians to simulate an approximate 20' x 20' x 8" deep field of sand. The modules were laid on a nominally horizontal surface of sand approximately 6 to 8 inches in depth at NREL's Outdoor Test Facility (PV CATS West Field, NE corner, see Figure 1) and connected to a Daystar MT5 Multi-Tracer IV system. The multi-tracer has a capacity of 16 modules; consequently, two HyET modules are connected in series and then connected to the multi-tracer. Daystar MT5 multi-tracer which permits measuring individual current-voltage (I-V) curves every 15 minutes, and between I-V curves the PV modules are peak- power tracked. The peak power and the voltage and current at peak power are measured every second and archived as one-minute averages. The associated parameters of plane-of-array irradiance (POA) and wind speed are also measured by the multi-tracer, as well as ambient air temperature, sand temperatures, geomembrane temperatures, and the backside temperatures of PV modules.

1.2.3. Module Outdoor Performance

Data has been taken from November 15, 2019, until August 30, 2021. Results presented here include two HyET modules connected in series, which we now refer to as a "PV Module" for consistency, which also describes how the multi-tracer channels were labeled for reporting purposes. Efficiencies are calculated based on the aperture area of the two HyET modules connected in series (15,120 cm^2).

Figure 1. 32 PV Modules installed at NREL's Outdoor Test Field

Months with frequent snow frequent snow falls reduced performance. Months without snow allowed for the performance of the PV modules to be more readily determined. For instance, Figure 2 shows daily efficiencies for PV Modules 12 through 15 for January 2020. These are the four PV Modules with the greatest power output and these efficiencies are obtained from the sums of the one-minute averages of peak power and POA. The other PV Modules are thought to have been damaged during installation or not representative of modules produced under consistent factory conditions. The daily POA values are included in Figure 4 and show the dependence of the efficiency on POA, indicating that the efficiency is less at low light levels. This is generally associated with a low shunt resistance of the PV device. For PV Modules 12 through 15, monthly efficiencies were 3.4%, 3.6%, 3.2%, and 3.7%, respectively.

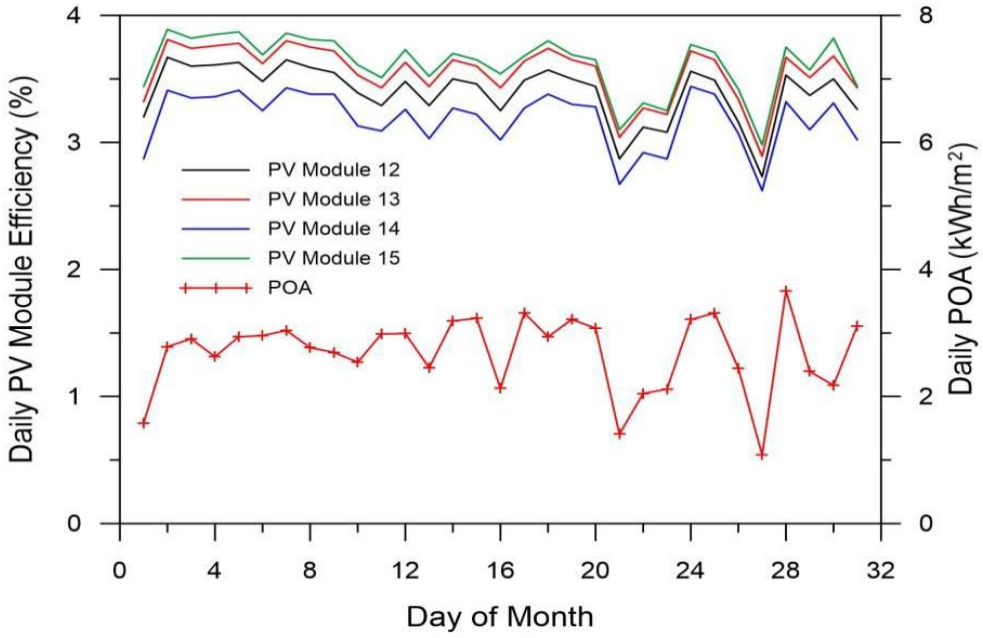

Figure 2. Daily efficiencies of PV Modules 12 through 15 for the month of January 2020. Efficiencies are shown to vary with the daily POA.

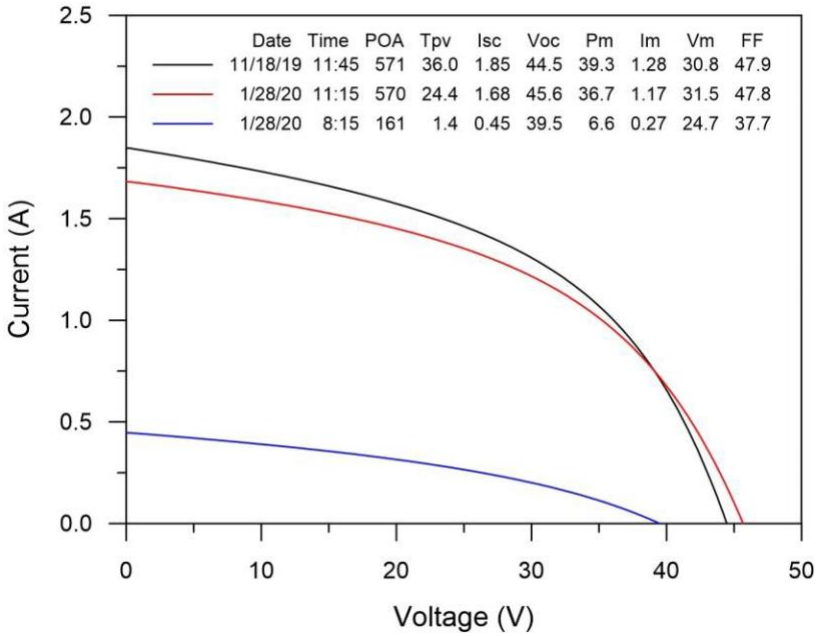

Figure 3. I-V curves for PV Module 15 showing changes in performance from November 18 to January 28 and dependency on light level on January 28. I-V curves measured under clear skies and tabular data shown for short-circuit current (Isc), open-circuit voltage (Voc), maximum power (Pm), current at maximum power (Im), voltage at maximum power (Vm), fill-factor (FF), PV module temperature (Tpv), and POA.

Figure 3 includes three I-V curves for PV Module 15. One on November 18 at 11:45; one on January 28^{t} at 11:15; and one on January 28 at 8:15. The first two I-V curves were measured under similar clear-sky conditions and POA about 10 weeks apart. Although the open-circuit voltage is greater because the PV module temperature is less, the latter I-V curve shows somewhat less output, perhaps from soiling, spectral effects, or because the light-induced degradation had not yet stabilized. The two I-V curves on January 28 further illustrate the output dependency on light level, as shown by the differences in fill-factor for the two I-V curves. Amorphous silicon PV modules have been shown to have a greater stabilized performance for warmer climates[i]; consequently, results obtained at NREL are not necessarily representative of other locations.

PV Module backside temperatures were measured with type T thermocouples labeled T_mod6, T_mod7, T_mod11, and T_mod15. These thermocouples were located between the geomembrane and backside of the PV modules and were used to calculate the irradiance-weighted PV temperature, $T_{i\text{-}w}$, and the PV temperature rise coefficient, T_{coef}.

The $T_{i\text{-}w}$ is useful for understanding how temperature effects may have influenced performance. It was calculated for January by dividing the sum of the products of PV Module temperatures and POAs by the sum of POAs. All the $T_{i\text{-}w}$ values were less than the Standard Test Condition (STC) temperature of 25°C; consequently, the temperatures in January should have been slightly beneficial with respect PV module efficiency. The variability of the $T_{i\text{-}w}$ values may be a consequence of the degree of contact between the geomembrane/PV module backsides and the sand surface below or the X-Y position in the group of PV modules.

The T_{coef} indicates the increase in PV Module temperature from ambient temperature when the POA is 1 kW/m^2. It was calculated for January by dividing the sum of the differences in temperatures between PV modules and ambient temperatures by the sum of POAs. Like T_{i-w} values, the variability in values may be a consequence of the degree of contact between the geomembrane/PV module backsides and the sand surface below or the X-Y position in the group of PV modules. The larger values are about the same as for a conventional rack-mounted PV module scenario.**Table 1. Irradiance-Weighted PV Temperature, T_{i-w}, and PV Temperature Rise Coefficient, T_{coef}, for January 2020.**

Thermocouple	Ti-w (°C)	Tcoef (°C/kW/m2)
T_mod6	18.3	24.6
T_mod7	17.9	23.1
T_mod11	16.5	20.2
T_mod15	14.7	16.5

NREL Personnel: Bill Marion, Bill Sekulic, Byron McDanold, Josh Parker

2. Task2: Yield properties of Power Foil:

2.1 Task Description

Power and energy yield performance data will be collected from the small-scale test station at NREL. These data will be compared to PV energy yield models using PV module parameters measured in NREL laboratories. Laboratory measurements will include temperature coefficients, spectral response, performance at standard test conditions, and performance over the International Electrotechnical Committee (IEC) 61853 irradiance-temperature matrix. NREL will implement best efforts under available scope of funding to derive diffuse and direct light sensitivity from field measurement data.

Field performance data of soil-mounted Power Foil modules will be referenced to standard crystalline silicon modules mounted in standard wind-blocking array at NREL's outdoor test facility.

2.2 Results

The purpose of this work is to derive the temperature coefficient, which is required to identify the reduction in conversion of the modules as a result of temperature increase. Overall, at the higher operating temperatures typical in high desert, the a-Si Power Foil shows a lower loss in energy yield as compared to conventional C-Si PV technology.

2.1.1. Experimental methods

Temperature Coefficients were determined at NREL, using a temperature control system that enables the measurement of I-V curves on PV devices over the temperature range 15 - 75 °C. The temperature control box consists of an insulated enclosure and a carriage which holds the device. Hot or cold air is directed around the device through the length of the box to control the temperature, and advanced algorithms based on feedback from an air temperature sensor and up to 16 thermal sensors fixed to the back of the device allow tight spatial and temporal temperature control. By placing the tool on a flash solar simulator *(Spire 5600 SLP* Pulsed Solar Simulator), the device is illuminated while within the enclosure.

The variation of the electrical parameters (or performance parameters) due to change in device temperature is a linear function. The slope of the linear regression is the absolute temperature coefficient (TC) reported in A/K for I_{sc}, V/K for V_{oc}, and W/K for P_{max}. The ratio of that slope value to the parameter's value (at 25°C, 1366.1 W/m^2, using the ASTM E490 reference spectrum) is defined as relative TC which is usually reported in %/°C or %/K. The relative temperature coefficient of I_{sc} is called α, the one of V_{oc} is called β, and the one of P_{max} is called γ, as obtained in (1). The temperature coefficients are extracted from the electrical parameters taken at different temperatures during the cooling down process (when the module temperature is uniform within ±2 °C according to IEC 60891).

$$a = \frac{1}{I_{sc}}\frac{dI_{sc}}{dT};\ b = \frac{1}{V_{oc}}\frac{dV_{oc}}{dT};\ g = \frac{1}{P_{\max}}\frac{dP_{\max}}{dT} \qquad (1)$$

2.1.2. Temperature Coefficients

Table 2. Relative temperature coefficient values for I_{sc}, V_{oc}, and P_{max}

Sample	Irradiance (W/m2)	α (%/°C)	β (%/°C)	γ (%/°C)
M1907-0019	1000	0.088	- 0.283	- 0.049 (range1)- 0.148 (range2) - 0.227 (range3)

I_{sc}, V_{oc}, and P_{max} as a function of temperature for the amorphous silicon are shown in figure 4 and Table 1 shows the relative temperature coefficients values for I_{sc}, V_{oc}, and P_{max}. The temperature coefficient for I_{sc} and V_{oc} are 0.088 %/°C and -0.283%/°C respectively. The amorphous silicon's temperature coefficient for P_{max} has three different slopes: −0.049 %/°C between 25°C to 30°C, −0.148%/°C between 30°C to 50°C and −0.227%/°C between 50°C to 75°C. What can be observed is that amorphous silicon has a significant advantage over crystalline silicon with regards to the temperature coefficient for Pmax (γ for c-Si is generally found between 0.3%/°C and 0.4%/°C in the literature).

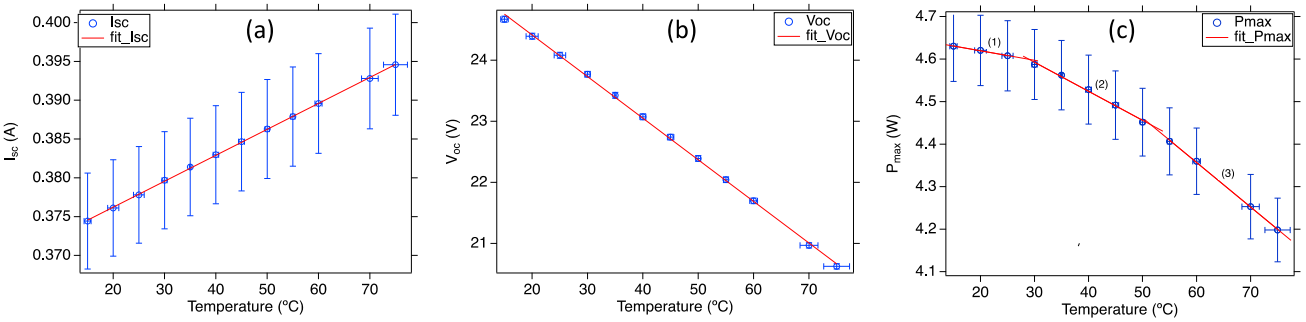

Figure 4. Temperature coefficients for (a) Isc, (b) Voc, and (c) Pmax for the a-Si from HyET.

2.1.3. Conclusion

Based on the study above, powerfoil may be more advantageous compared to crystalline silicon panels at high operating temperatures (e.g., solar farms in desert environments) and lead to a higher energy yield.

3. Task3: Reliability / durability assessment of HyET Power Foil PV Modules and various base polymer membranes

3.1. General Task Description

For over five decades, field results have shown that the combinations of the stress factors of the natural environment have markedly greater impact than separate, factor-specific laboratory tests. Application of stress levels in a balanced combination appropriate to the natural environment will thus reduce test time, while also avoiding costly over overdesign. With NREL's combined-accelerated stress testing protocol (C-AST) new materials and components assembled in the mini-module platform are tested for durability using simultaneous, combined accelerated stress testing based on a weathering platform. This permits the examination of PV module durability more quickly, reliably, and with fewer samples for truly field-relevant testing. With this capability, we can combine the environmental stress factors including light, temperature, humidity, rain/spray, system voltage, and mechanical stress (thermo-mechanical and static loading) [*note mechanical stress omitted in this proposal*]. Combining the stress factors of the natural environment, with fewer modules, fewer parallel tests, it is possible to discover mechanisms not a-priori known in new module designs, reduce residual risk, potentially accelerate time to market and bankability, and reduce costly overdesign.

Reliability and durability assessment will be performed according NREL's combined-accelerated stress testing protocol, based on ASTM-D7869. This protocol was originally designed to replicate paints & coatings failures with 8 x - 16 x acceleration factor (Florida USA baseline) and was further developed by NREL for the evaluation of photovoltaic modules.

3.2 Stress levels: experiments conducted in NREL's multi-stress environmental chamber

- Heat (-20°C to 90°C)
- Full spectrum light (approximately 2-sun, intermittent)
- Humidity (Condensing, Non-condensing)
- System voltage stress optional
- Modules will be connected to a load resistor to roughly approximate average Pmax loading
- Short periods of lower temperature will be applied (-40°C) to ensure survivability at low temperature

3.3 Samples and duration

- 2 samples, sample size up to approximately 33 cm x 33 cm
- Approximately 5 months of test, simulating at least 5 y in the field in hot/humid tropical climate, based on the ASTM D7869 test protocol, modified for testing of PV modules.

3.4 Measurement and evaluation

- 2-week observation interval (flash test, visual inspection)
- Periodic optical and electroluminescence imaging.

Stabilization will be performed to IEC 61215: 2016 to achieve stability before the start of testing. Because the C-AST is performed under light, additional (separate) stabilization procedures will not be performed over the course of the testing.

3.5 Reporting

- One interim and one final report will be provided. The report will consist of running biweekly power performance measurements, results of visual inspection, images, comments, and recommendations.

3.2. Results

3.2.1. Combined-accelerated stress test protocol

Below is described the methodology of Combined-Accelerated Stress Testing (C-AST), a discussion of the HyET modules tested (including preconditioning for metastability, test results, and a brief discussion about them. The combined-accelerated stress test (C-AST) protocol developed by NREL [1, 2] combines multiple stress factors including full-spectrum light, temperature, humidity, mechanical loading, system voltage and rain spray. C-AST has previously been reported to successfully reproduce field-failures in several backsheet types [3]. Furthermore, the reproduced failure mechanisms have been shown to be field-relevant, and not the result of any unrealistic stress application because the C-AST protocol applies stress levels no higher than that of the natural environment and in realistic combinations [4]. Acceleration is achieved by applying the stress levels at the statistical tails that the product experiences in the natural environment. The C-AST protocol consists of multiple phases. Tropical is a largely a high-humidity, high-temperature protocol based on ASTM D7869, which was designed to replicate environmental conditions observed in South Florida. Additional segments are designed to test for environmental conditions not observed in tropical environments, capturing the extremes of Winter, Spring, and High Desert. It includes low-humidity protocols with extended periods and of low and high temperature with the inclusion of some intensive thermal cycling, along with the aforementioned stress factors (Fig. 5). ASTM D7869, on which the tropical protocol is based, has an average acceleration factor of about 12 x for different paints and coatings tested in the south Florida environment [5]. We however modified ASTM D7869 for PV modules. We have seen polyamide backsheet fail in the Tropical C-AST test with an acceleration factor of about 14 x over Albuquerque, New Mexico [3].

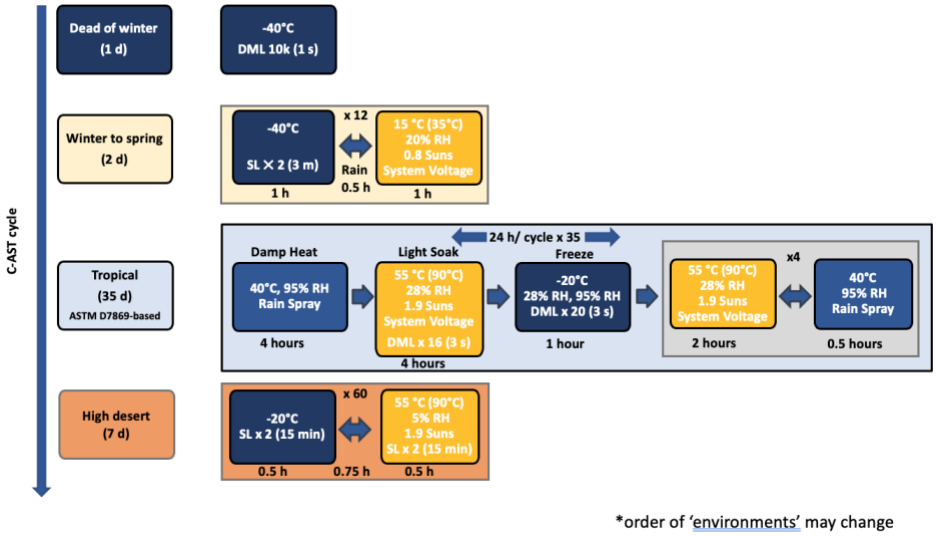

Figure 5. Schematic of C-AST stress protocols.

Two HyET modules of effective area 852.3 cm^2 were stabilized according to IEC 61215, under approximately 1000 W/m^2 at 50 °C for a total of 156 h.

Final flash test measurements after the stabilization process are according to Table 3.

Table 3. IEC 61215-stabilized cell properties as determined by a SPIRE 5600 under standard test condition (1000 W/m², 25°C) and at low light (200 W/m², 25°C).

NREL ID	Sample ID	date	Irr (W/m²)	Voc (V)	Isc (A)	FF (%)	Vmax (V)	Imax (A)	Pmax (W)
M1908-0013	1801510988-95	9/20/19	1000	24.684	0.402	55.04	17.77	0.3078	5.4686
M1908-0013	1801510988-95	9/20/19	200	21.986	0.073	54.57	16.146	0.0548	0.8843
	1801511153-90	9/20/19	1000	24.695	0.407	54.58	17.345	0.3168	5.4949
M1908-0014	1801511153-90	9/20/19	200	21.885	0.074	58.42	16.411	0.0579	0.9507

3.2.2. Testing

Data has been taken from October 9, 2019, until December 31, 2021. An example of 2 months testing through CAST is shown on table 2.

Testing through C-AST was performed according to Table 4. To date, slightly under 2 months of an intended 5 months of stress testing was applied.

Table 4. Testing schedule of two HyET solar modules through combined accelerated stress testing.

CAST Sequence	Duration	Cycles	Characterization	Stress Start	Stress Complete	Stress Time (MO)		Days/Month
Spring-01	36hr	12	none	10/9/19	10/11/19	0.06575342		30.42
High Desert-01 (R1)	1wk	60	Imaging/IVs	10/11/19	10/18/19	0.23013699		
								Total Stress Time (Months)
Dead of Winter-1	5-18hr	soak	~~Imaging only~~	11/5/19	11/6/19	0.03287671		1.96
Spring-1a (R2)	36hr	12	Imaging/IVs	11/6/19	11/8/19	0.06575342		
Tropical-1a (R3)	2.5wk	17.5	Imaging/IVs	11/12/19	12/2/19	0.65753425		
Tropical-1b (R4)	2.5wk	17.5	Imaging/IVs	12/21/18	1/8/19	0.57534247		
High Desert-1 (R5)	1wk	60	Imaging/IVs	1/11/20	1/21/20	0.32876712		
Dead of Winter-2	5-18hr	soak	Imaging only			0		
Spring-2 (R6)	36hr	12	EL/IVs/visual Inspection			0		
Tropical-2a (R7)	2.5wk	17.5	Imaging/IVs			0		
Tropical-2b (R8)	2.5wk	17.5	Imaging/IVs			0		
High Desert-2 (R9)	1wk	60	Imaging/IVs			0		

3.2.3. Outcome

Flash test results at interim pulls of the module after most of the stages of the stress testing listed in Table 3 normalized to their initial values enumerated in Table 1 are displayed in Fig. 6. Flash tests were performed immediately after the end of test cycles to minimize changes to metastability state between the end of stress testing and the flash testing.

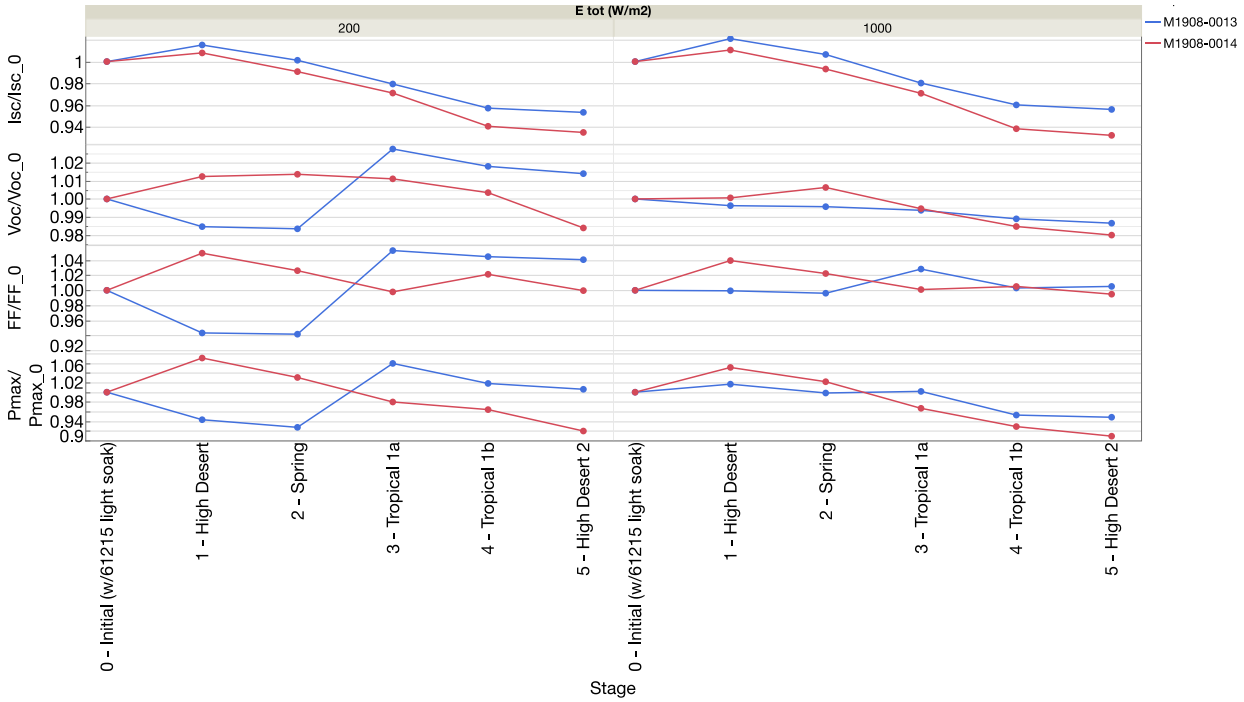

Figure 6. Flash test results at two irradiance levels as indicated for two HyET modules (25°C). Flash tests are taken after the stages indicated on the horizontal axis and correspond to flash tests after C-AST sequence rounds (R) indicated in Table 3.

3.2.4. Discussion

The samples were initially stabilized at stage 0 and not at any other subsequent stages. It is therefore most meaningful to compare where possible samples after similar test stage types. The only case this applies in the data so far is after stage 1 and 5, both High Desert.

Examining the short circuit current, I_{sc} in Fig. 6, we can see a fall totaling about 6% relative over the course of the C-AST exposure. There is no difference in the 1000 W/m^2 and low light 200 W/m^2 degradation percentage in I_{sc}, indicating there is no light-injection-dependent effect. The degradation may be associated with humidity because the degradation occurs predominantly in the high humidity containing sequences.

Fill factor did not degrade significantly at 1000 W/m^2, indicating no important rise in series resistance. Fill factor (FF) under low light oscillated a great deal, which was found to relate to shunts in the connections between the laser-isolated cells forming and burning out. These oscillation in FF were not seen in 1000 W/m^2 data because the shunt paths tend to saturate in full light (the shunt formation and burning out could be seen in the electroluminescence images of the modules, not shown here).

Degradation in open circuit voltage (V_{oc}) is 1 % to 2 % (relative) at 1000 W/m^2 over the course of test. If the 6% degradation were to be completely associated with optical losses due to opacity or scattering in the polymeric superstrate (a likely but not proven cause), the associated fall in V_{oc} would be about 0.5 % based on previously published relationships [6]. Since we see greater fall than 0.6 %, the reminder of the open circuit voltage loss may be associated with minority carrier lifetime loss. Overall power loss over the course of testing is about 7% at standard test conditions. We will not know until after the IEC 61215 light stabilization procedure is done again at the end of the stress testing what the light stabilized power losses will be compared to the initial light stabilized power.

References:

[1] S. Spataru, P. Hacke, and M. Owen-Bellini, "Combined-Accelerated Stress Testing System for Photovoltaic Modules," in *Proceedings of 45th IEEE Photovoltaics Specialists Conference*, 2018.

[2] M. Owen-Bellini, P. Hacke, S. Spataru, D. C. Miller, and M. D. Kempe, "Combined-Accelerated Stress Testing for Advanced Reliability Assessment of Photovoltaic Modules," in *35th European PV Solar Energy Conference and Exhibition*, 2018.

[3] P. Hacke *et al.*, "Combined and sequential accelerated stress testing for derisking photovoltaic modules," in *Advanced Nano- and Micro-materials for Photovoltaics: Future and Emerging Technologies*, Amsterdam: Elsevier, 2019.

[4] M. Owen-bellini *et al.*, "Correlation of advanced accelerated stress testing with polyamide-based photovoltaic backsheet field-failures," in *46th IEEE Photovoltaics Specialist Conference*, 2019.

[5] Nichols *et al.* "An improved accelerated weathering protocol to anticipate Florida exposure behavior of coatings," J. Coat. Technol. Res. DOI 10.1007/s11998-012-9467-x

[6] K. Thongpao *et al.* "Outdoor performance of polycrystalline and amorphous silicon solar cells based on the influence of irradiance and module temperature in Thailand" In ECTI-CON2010: The 2010 ECTI International Confernce on Electrical Engineering/Electronics, Computer, Telecommunications and Information Technology 2010 May 19 (pp. 74-77). IEEE.

Subject Inventions Listing:

None

ROI #:

None

[i] Ruther et al., "Performance Test of Amorphous Silicon Modules in Different Climates – Year Four: Progress in Understanding Exposure History Stabilization Effects," 33rd IEEE PVSC, 2008. https://www.nrel.gov/docs/fy08osti/42523.pdf